Title

The International Bathymetric Chart of the Arctic Ocean Version 4.0.

Journal

Scientific data, 7(1)

ISSN

2052-4463

Authors

Jakobsson, Martin
Mayer, Larry A
Bringensparr, Caroline
et al.

Publication Date

2020-07-01

DOI

10.1038/s41597-020-0520-9

Peer reviewed

SCIENTIFIC DATA

OPEN

DATA DESCRIPTOR

The International Bathymetric Chart of the Arctic Ocean Version 4.0

Martin Jakobsson *et al.*[#]

Bathymetry (seafloor depth), is a critical parameter providing the geospatial context for a multitude of marine scientific studies. Since 1997, the International Bathymetric Chart of the Arctic Ocean (IBCAO) has been the authoritative source of bathymetry for the Arctic Ocean. IBCAO has merged its efforts with the Nippon Foundation-GEBCO-Seabed 2030 Project, with the goal of mapping all of the oceans by 2030. Here we present the latest version (IBCAO Ver. 4.0), with more than twice the resolution (200 × 200 m versus 500 × 500 m) and with individual depth soundings constraining three times more area of the Arctic Ocean (~19.8% versus 6.7%), than the previous IBCAO Ver. 3.0 released in 2012. Modern multibeam bathymetry comprises ~14.3% in Ver. 4.0 compared to ~5.4% in Ver. 3.0. Thus, the new IBCAO Ver. 4.0 has substantially more seafloor morphological information that offers new insights into a range of submarine features and processes; for example, the improved portrayal of Greenland fjords better serves predictive modelling of the fate of the Greenland Ice Sheet.

Background & Summary

A broad range of Arctic climate and environmental research, including questions on the declining cryosphere and the geological history of the Arctic Basin, require knowledge of the depth and shape of the seafloor[1–3]. Bathymetry provides the geospatial framework for these and other studies[4] and has impact on many processes, including the pathways of ocean currents and, thus, the distribution of heat[5,6], sea-ice decline[7], the effect of inflowing warm waters on tidewater glaciers[8], and the stability of marine-based ice streams and outlet glaciers grounded on the seabed[9–11]. Bathymetric data from large parts of the Arctic Ocean are, however, not available or extremely sparse due to difficulties, both logistical and political, in accessing the region[12].

The International Bathymetric Chart of the Arctic Ocean (IBCAO) project, was initiated in 1997 in St Petersburg, Russia, to address the need for up-to-date digital portrayals of the Arctic Ocean seafloor[13]. Since 1997, three Digital Bathymetric Models (DBMs) have ingested new data sets compiled by the IBCAO project team and have been released for public use[14–16]. These DBMs comprised grids with a regular cell size of 2.5 × 2.5 km (Ver. 1.0), 2 × 2 km (Ver. 2.0) and 500 × 500 m (Ver. 3.0) on a Polar Stereographic projection. Depth estimates for grid cells between constraining depth observations were interpolated by the continuous curvature spline in a tension gridding algorithm[17]. All depth data available at the time of the compilations were used, including multi- and single-beam bathymetry, and contours and soundings digitized from depth charts, with direct depth observations having the highest priority and digitized contours the lowest[18].

Recognizing the importance of complete global bathymetry, the General Bathymetric Chart of the Ocean (GEBCO), a project under the auspices of the International Hydrographic Organization (IHO) and the Intergovernmental Oceanographic Commission (IOC), teamed up with the Nippon Foundation of Japan and jointly launched the Seabed 2030 project in 2018 with the goal of mapping all of the world ocean by 2030[19]. The first release from the Seabed 2030 project was the *GEBCO_2019* global grid, with a grid-cell size of 15 × 15 arc seconds[20]. The Arctic Ocean is poorly represented by this geographical grid because the grid cells are greatly distorted in the longitudinal direction at high latitudes. Seabed 2030 is built on the IBCAO model; a focused effort to gather and assemble all available bathymetric data into a digital database that is then used to compile a DBM. Seabed 2030 has established four Regional Centers, one of which (shared by Stockholm University and the University of New Hampshire) has responsibility for the Arctic Ocean. With the establishment of Seabed 2030,

[#]A full list of authors and their affiliations appears at the end of the paper.

the IBCAO has merged its efforts with Seabed 2030 and, while keeping its well-established identity, the compilation of updated versions of IBCAO will now be conducted under the auspices of the Seabed 2030 Arctic Regional Center.

Here we present IBCAO Ver. 4.0, incorporating new data sources and compiled using an improved gridding algorithm and with a finer grid-cell size of 200 × 200 m on a Polar Stereographic Projection. Recognizing that the lateral resolution achievable by a surface-ship deployed echo-sounder varies as a function of depth (decreasing resolution with depth), the Seabed 2030 project has defined target grid-cell sizes that are also variable by depth[19] (see Methods Section). The data coverage within the Ver. 4.0 area is therefore calculated with respect to the Seabed 2030 target resolutions. In total, ~19.8% of the gridded area is constrained by some form of bathymetric data, excluding digitized bathymetric contours, whereas the comparable coverage for IBCAO Ver. 3.0 was calculated as ~6.7% (Fig. 1) using the variable resolution grid. Ver. 4.0 has ~14.3% of the gridded area comprised of modern multibeam echo-sounder derived bathymetry whereas Ver. 3.0 had ~5.4%. This implies that the new Ver. 4.0 has ~2.7 times the area of the Arctic Ocean constrained by multibeam bathymetry relative to Ver. 3.0. One of the important additions to IBCAO Ver. 4.0 is the recently released IceBridge BedMachine Ver. 3 topography/bathymetry grid of Greenland[21], containing both Greenland ice-surface and under-ice topography, yielding a seamless transition to the adjacent seafloor along most of the margins of the Greenland Ice Sheet, which is critical for ice-sheet modelling and for improving projections of the impact of Greenland on future sea level rise. The IBCAO DBM will be updated continuously as new data become available.

Methods

Grid compilation. The IBCAO DBM compilation workflow, illustrated schematically in Fig. 2, contains six main steps. Step 1 consists of assembling the different kinds of contributed depth data listed in Table 1 along with necessary metadata. The metadata follow the standard adopted by EMODnet Bathymetry[22], with the additions shown in Online-only Table 1. Contributions to IBCAO come in various forms. Ideally, contributions are cleaned bathymetric data in the form of XYZ points representing spot soundings, single-beam soundings, nodes of high-resolution multibeam grids, or nodes of digitized contours from bathymetric maps. Gridded compilations derived from multiple sources have also been contributed (see sub-section 'Source data' and Online-only Table 2; the latter only available online) as well as raw multibeam bathymetry requiring processing. All gathered XYZ datasets are reviewed using QPS Qimera software. If necessary, additional post-processing is applied in Step 2 using tools available in Qimera including, for example, removal of outliers or adjustments of vertical levels where systematic offsets are evident. If datasets of relatively poor quality are found to be in conflict with other observations, they may be completely or partially removed. In Step 3, additional metadata are included; most importantly the version number of each dataset is incremented if it has been modified, permitting roll-back through the processing history.

In Step 4, the processed XYZ data are gridded using a modified version of the algorithm applied to compile IBCAO Ver. 3.0[15]. First, a low-resolution grid with a cell-spacing of 2000 × 2000 m is produced. The depth data passed forward are selected based on their quality prioritization within each 2000 × 2000 m grid cell. Multibeam data are generally prioritized before single-beam and spot-sounding data which, in turn, are prioritized ahead of digitized depth contours from charts. A block median filter is then applied using the Generic Mapping Tools (GMT)[23]. The block median filtered data are subsequently gridded using the GMT routine *surface*, which applies a continuous curvature spline in tension function[17]. The tension parameter is set to 0.34. This value was decided on after analyses of the gridding results over the course of the IBCAO-project. A value of 0 implies no tension of the spline surface, whereas a tension of 1 removes the curvature altogether by not permitting maxima or minima between constraining data points. The resulting 2000 × 2000 m grid is smoothed using a cosine filter over 6000 m in GMT to provide a smooth base over which higher-resolution data are merged. The smoothed grid is then resampled to 100 × 100 m.

Higher resolution datasets (i.e. multibeam surveys and some gridded compilations) are individually down-sampled (if high enough in resolution) to 100 × 100 m. If multiple contrasting depths exist for one grid cell, the depths passed forward to the block median filter at 100 × 100 m are selected based on the same prioritization as used for the 2000 × 2000 m grid cells. The final step in the preparation of the high-resolution data consists of a density filter, which only passes forward data if more than 30% of an area of 1000 × 1000 m is covered by depth values.

The final action within Step 4 consists of merging the high-resolution data passed forward from the procedure described above with the 100 × 100 m resampled 2000 × 2000 m smoothed grid by applying a remove-and-restore approach[24]. This involves the calculation of the difference between the 2000 × 2000 m grid resampled to 100 × 100 m and the high-resolution 100 × 100 m datasets remaining after applying the density filter. The differences, or residuals, are then gridded using the surface spline in tension function before they are added back onto the low-resolution 2000 × 2000 m grid (resampled to 100 × 100 m). This procedure results in a smooth merging of the high-resolution data onto the low-resolution resampled grid. To prevent introducing spline-function artifacts, the residuals are forced to be zero at a distance of 1000 m from the data. Finally, the entire grid is resampled to 200 × 200 m. The gridding algorithm is written in Python, from which the applied GMT routines are called.

Step 5 consists of a quality check of the final grid using a Stockholm University developed web interface along with Qimera and the Open Source Geographic Information System QGIS, version 3.8.3-Zanzibar, which has also been used to produce the maps displayed in this data description[25]. The web interface has a mark-up function permitting all members in the IBCAO Regional Mapping Committee to take part in the quality control. If issues are found and marked, the associated source data are passed back to Step 2 for further analysis and processing. Step 6 in Fig. 2 is described in the following sub-section.

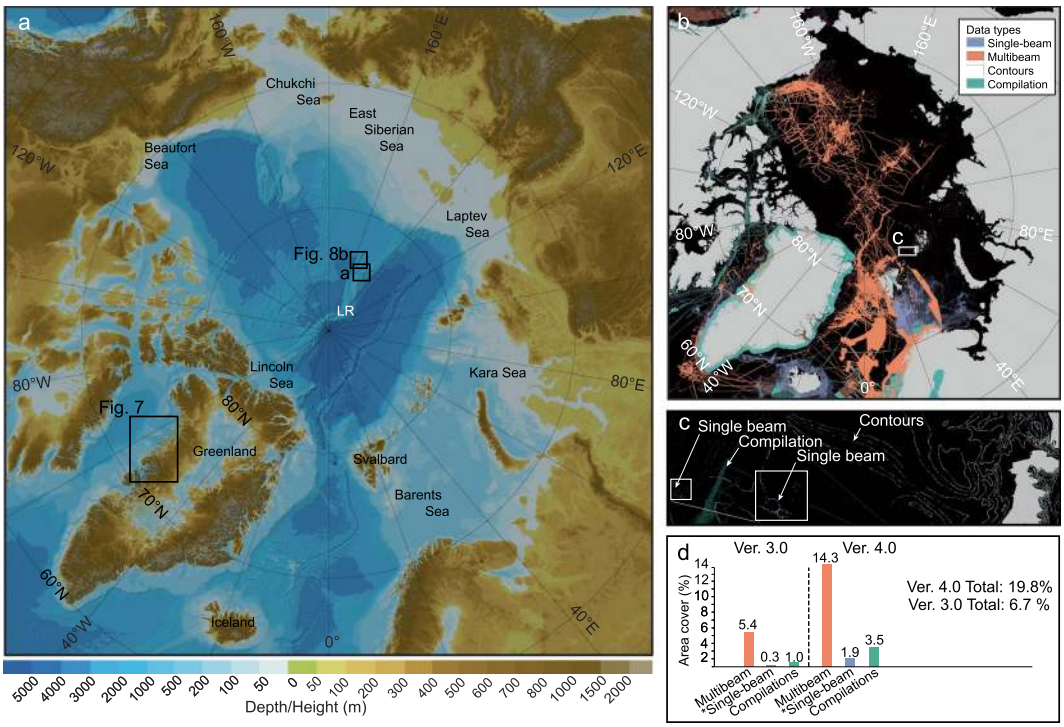

Fig. 1 **(a)** Shaded relief map of IBCAO Ver. 4.0 with the under-ice topography of Greenland from BedMachine Ver. 3 shown. **(b)** Map of Ver. 4.0 data sources grouped into the data types (TID) listed in Table 1. **(c)** Close-up showing an area with single-beam soundings and digitized depth contours used in gridding. Since these data types occupy relatively few grid cells, they are difficult to see in the overview map shown in **(b)**. **(d)** Summary statistics of the proportion of the IBCAO area covered by the different data types in Ver. 4.0 and 3.0. The data types "steering points" and "interpolated depths" are not shown in **(a)** as they are not counted as part of the depth data (Methods; Table 1). *Refers to "Isolated soundings", "ENC soundings" and "Mixture of direct measurement methods", which are merged with data type "Single-beam" sounding on the map as well as in the summary statistics shown in (**d**). LR: Lomonosov Ridge.

Calculation of statistics. Echo sounders mounted on surface vessels increase their ensonified area with increasing depth, thus decreasing their achievable mapping resolution with depth. Based on this principle, Seabed 2030 defined a set of target mapping resolutions: 0–1500 m, 100 × 100 m; 1500–3000 m, 200 × 200 m; 3000–5750 m, 400 × 400 m; and 5750–11000 m, 800 × 800 m[19]. Since IBCAO contributes to the Seabed 2030 project, the data coverage calculated in Step 6 uses the Seabed 2030 resolutions. For example, a depth sounding between 3000–5750 m is considered to map an area of 400 × 400 m whereas a sounding with a value between 0–1500 m only maps an area of 100 × 100 m. Where the source data are available in the form of multibeam, single-beam and spot soundings, it is thus relatively easy to calculate how much of the IBCAO grid is mapped or not. However, when the contributed data are compilation grids, the estimated surveyed area is uncertain as we do not know the underlying data coverage. Even if only the nodes of the contributed grids at their native resolution (i.e. before resampling) are counted, they will likely overestimate the mapped area. For this reason, gridded compilations are kept as a separate category (Fig. 1).

Data Records

Source data. The IBCAO Ver. 4 is available for download from the British Oceanographic Data Centre[26]. The bathymetric source data for IBCAO Ver. 4 are listed in Online-only Table 2 along with references where available. Individual surveys are, in most cases, aggregated to one contributing organization. Each dataset is assigned a Source Identification number (SID) and Type Identification number (TID). The former links each dataset to its full metadata whereas the latter groups the data into the categories listed in Table 1. SID and TID grids are compiled within the workflow in Fig. 2 (See SID and TID maps in Figs. 3 and 4). Spatially, the largest contributed gridded compilations are BedMachine Ver. 3 covering the coastal waters of Greenland[21], MAREANO mapping a significant portion of the Norwegian EEZ, EMODnet encompassing European Arctic waters, including the part of Bay of Bothnia covered by IBCAO[22], and NONNA-100 composed of bathymetric data from Canadian waters released by the Canadian Hydrographic Service at a resolution of approximately 100 m. BedMachine Ver. 3 also provides the under-ice topography of Greenland at a gridded horizontal resolution of 150 m, derived from ice-thickness measurements from NASA's Operation IceBridge and other surveys using ice-penetrating radar and an ice-mass conservation algorithm in the coastal areas[21]. The bathymetry in BedMachine Ver. 3 is, for the most part, linked back to IBCAO Ver. 3.0, RTopo-2[27] and the DBM by Arndt, *et al.*[28] of northeastern Greenland, apart

TID	Data type	Description
10	Singlebeam	Depth value collected by a singlebeam echo-sounder
11	Multibeam	Depth value from grid derived from multibeam echo-soundings
17	Combination of direct measurement methods	Depth values from single beam, spot sounding or a combination of other direct measurements. Crowd sourced bathymetry from, for example Olex, falls under this category
41	Interpolated based on a computer algorithm	Depth value is an interpolated value based on a computer algorithm (e.g. spline in tension). These are counted as no data in statistics describing coverage
42	Digital bathymetric contours from charts	Depth values taken from digitized bathymetric contours
70	Pre-generated grid	Depth value is taken from a pre-generated grid that in turn is based on mixed source data types (e.g. single beam, multibeam, interpolation etc.)
72	Steering points	Depth value used to constrain the grid in areas of poor data coverage. These are counted as no data in statistics describing coverage
13	Isolated sounding	Depth value that is not part of a regular ship survey or trackline, (e.g. spot soundings through sea ice)
14	ENC sounding	Depth value extracted from an Electronic Navigation Chart (ENC)

Table 1. The source data used in the IBCAO Ver. 4.0 compilation classified into data types (TID; Type Identification). In the calculated statistics of mapped area, types 13, 14 and 17 are included in type 10 whereas 41 and 72 are counted as no data.

from within the fjords where a kriging algorithm is used to interpolate depths between the under-ice topography and available bathymetric data, including recent surveys along the Greenland coastline carried out by the NASA Earth Venture Suborbital mission named Oceans Melting Greenland[8,29]. We have masked BedMachine Ver. 3 so it is used from the outer coast of Greenland, resulting in a vastly improved fjord representation compared with other bathymetric models. Bathymetric data from Greenland coastal waters gathered since BedMachine Ver. 3 have been merged using the remove-and-restore approach. These include, for example, multibeam surveys of Petermann and Sherard Osborn fjords in northwest Greenland[30] and additional bathymetry collected and compiled within NASA's Ocean Melting Greenland[31,32].

The area covered by "crowd sourced" bathymetry has increased substantially in Ver. 4.0 compared to Ver. 3.0 through contributions from fishing vessels and other ships using Olex (www.olex.no) and MaxSea (http://www.maxsea.com/) mapping systems, the latter in Greenland waters only. Since 2012, when IBCAO Ver. 3.0 was compiled, numerous icebreaker expeditions mapping the seafloor with multibeam sonar in the sea-ice covered Arctic Ocean have been completed. These include expeditions with Canadian CCGS *Amundsen* and CCGS *Louis S. St-Laurent*, German RV *Polarstern*, Swedish icebreaker *Oden*, and USCGC *Healy* (Online-only Table 2).

Technical Validation

Validation: Comparison between IBCAO Vers. 3.0 and 4.0. The improvements in IBCAO Ver. 4.0 compared to earlier versions result from the large amount of new bathymetric data including gridded compilations, an improved gridding algorithm, and a higher resolution. This is best illustrated by specific examples, together with an overview map showing the depth differences between IBCAO Vers. 3.0 and 4.0, generated by subtracting Ver. 3.0 from 4.0, that highlights the most significantly updated areas (Fig. 5). The new multibeam bathymetry is readily visible in the difference map as well as in the improved representation of fjords along sections of the Greenland coast (Fig. 5). In general, the least updated areas in terms of absolute depth changes are located on the Russian continental shelf, in the Barents Sea between southern Svalbard and northern Norway, and on the Norwegian and Iceland continental shelves (Fig. 5). The lack of updates in Russian waters stems from the fact that no new multibeam data has been contributed from these areas, despite their collection during Russian efforts to map the extent of their juridical continental shelf. If we look at the updates as a function of how much the depth has changed relative to water depth (i.e. the percent depth change), the East Siberian and Laptev seas show some clear differences in Ver. 4.0 compared to 3.0 (Fig. 6). The updates result from the fact that individual soundings on charts were used, rather than digitized contours from charts, providing more bathymetric detail (Fig. 6). These soundings were digitized by Danielson, *et al.*[33] for the purpose of compiling the Alaska Region Digital Elevation Model (ARDEM). Areas that do not show large depth differences were already relatively well

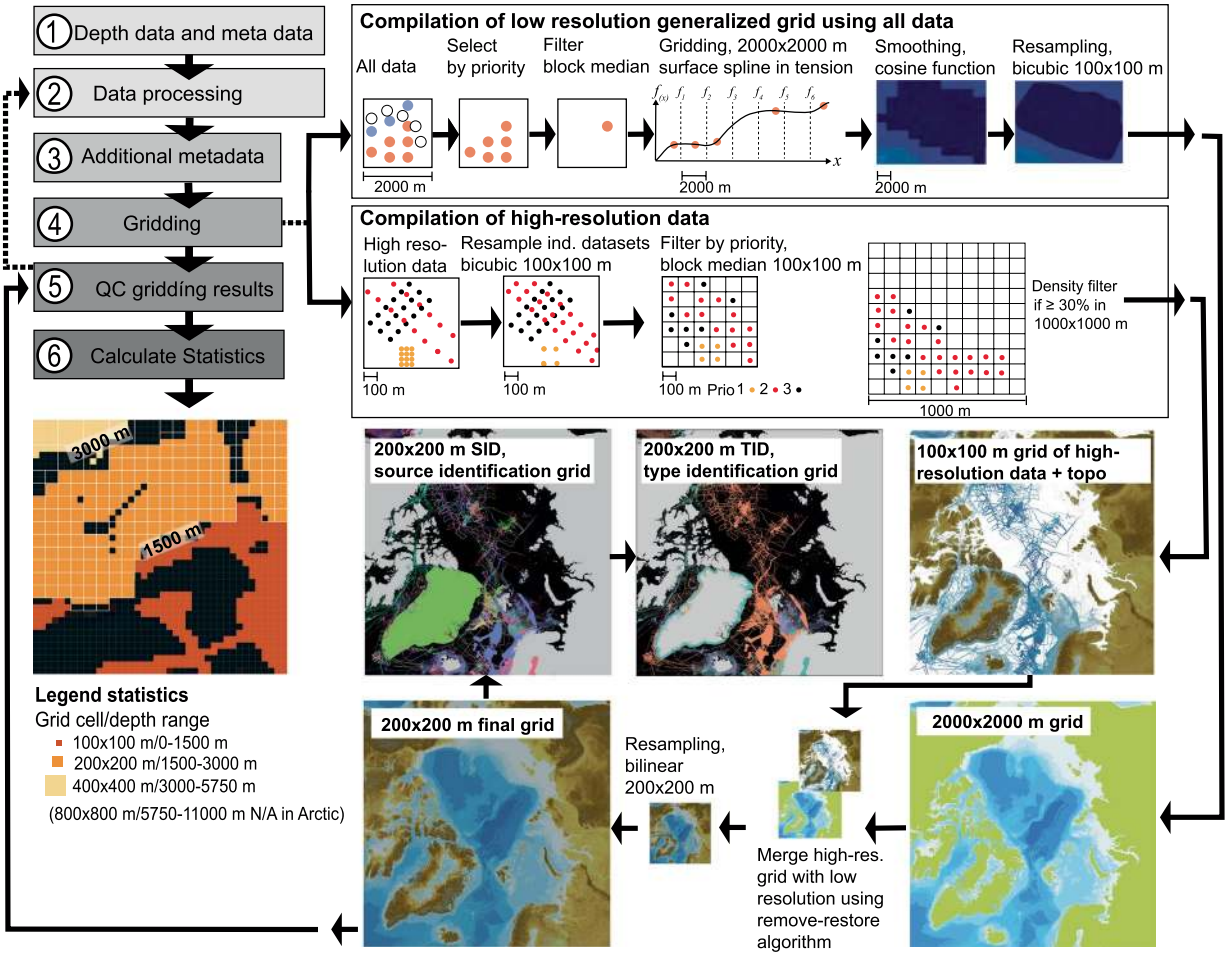

Fig. 2 Schematic illustration of the IBCAO DBM compilation work flow.

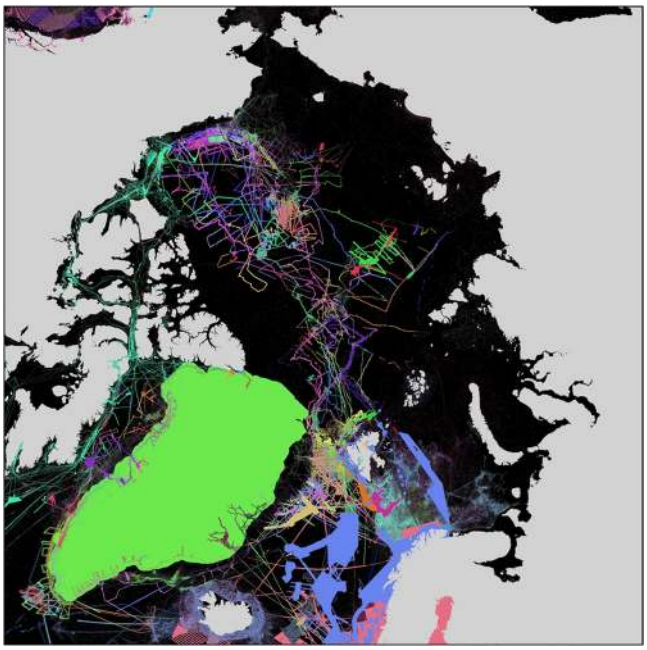

Fig. 3 Map showing the underlying sources for IBCAO Ver. 4 based on the Source Identification grid (SID) available for download. The source of the depth used within a specific 200 × 200 m grid-cell in the gridding is linked by a unique number to a database record containing the source metadata. Legend is not included as there are 505 SIDs.

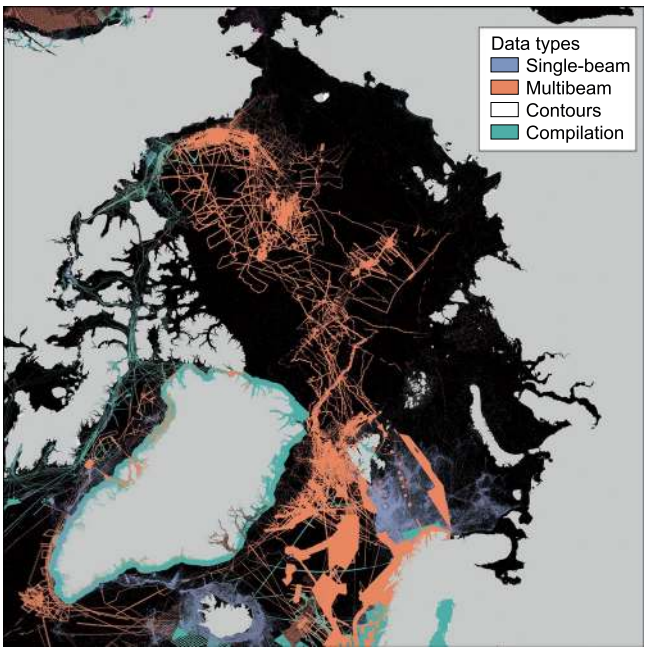

Fig. 4 Map showing the underlying sources for IBCAO Ver. 4 classified into the data types listed in Table 1. "Isolated soundings", "ENC soundings" and "Combination of direct measurement methods" listed in Table 1 are merged with data type "Single-beam" in this map. Note that contours and single-beam soundings hardly show at this scale.

mapped in IBCAO Ver. 3.0. If the Barents Sea is examined carefully, the new additions from the MAREANO compilation are clearly visible (Fig. 5).

The incorporation of BedMachine Ver. 3 and additional merging of all bathymetry available since its release not only enhances the representation of Greenland fjords, but also highlights the complex coastal bathymetry (Fig. 7). This is particularly noticeable off the western coast of Greenland between about 55°N and 75°N, where IBCAO Ver. 4.0 reveals a rough submarine landscape characterized by criss-crossing channels that commonly occur where the seafloor is composed of igneous bedrock (Fig. 7). The transition to a smoother seafloor morphology on the outer continental shelf occurs rather abruptly across a near straight southwest-to-northeast trending line that fits well with geological maps showing change across a thrust fault from igneous rocks to a seafloor composed of sedimentary rocks further offshore[34] (Fig. 7).

Lack of depth data from the western Greenland inner continental shelf in IBCAO Ver. 3.0 resulted in a poorly constrained spline function causing undulations that do not represent the "true" seafloor morphology in this area (Fig. 7b). The Uummannaq Fjord of western Greenland is a good example, showing that submarine glacial landforms with spatial dimensions on the order of hundreds of meters, such as glacially streamlined drumlins and large mega-scale glacial lineations images using multibeam, are distinguishable in the IBCAO Ver. 4.0 DBM (Fig. 7d). This can only be the case when the gridding is based on high-resolution bathymetry, here collected by RRS *James Clark Ross*[35].

The Lomonosov Ridge extends >1600 km across the central Arctic Ocean between the continental shelves of Northern Greenland and Siberia (Fig. 1). Details of the ridge came to light in the first published version of IBCAO[16] where it was drastically remapped compared to the GEBCO Sheet 5.17[36], which had served as the authoritative international bathymetric map of the Arctic Ocean for nearly two decades before the IBCAO project began. Numerous multibeam surveys with icebreakers have been carried out over the Lomonosov Ridge since the release of IBCAO Ver. 3.0, (Online-only Table 2), leading again to a substantially improved bathymetry (Fig. 8). Examples include surveys that have been individually published revealing critical sills that influence water exchange across the Lomonosov Ridge[6], ice-shelf grounding on the ridge crest[37], and where the foot of the slope is located along the ridge flanks, identified for the purpose of substantiating Denmark's submission under Article 76 of the United Nations Convention on the Law of the Sea (UNCLOS)[38].

The Science Ice Exercise (SCICEX) was a program utilizing US Navy nuclear submarines for systematic mapping under the Arctic Ocean pack ice between 1993 and 2001[39]. Of the eight completed expeditions, two (1998 and 1999) involved acquisition of swath bathymetry using the specifically designed sonar system Seafloor Characterization and Mapping Pod (SCAMP)[39]. This swath bathymetry was used in IBCAO Ver. 3.0, although in many areas newer multibeam bathymetry has now replaced the SCICEX data; for example along the Northern Alaskan margin and on Chukchi Borderland, where several mapping expeditions with USCGC *Healy* have been carried out to collect seafloor bathymetry in support of the establishment of a U.S. extended continental shelf under Article 76 of UNCLOS[40]. A major caveat with SCICEX/SCAMP data has been the problem of precisely geo-registering the swath bathymetry, which is particularly evident where areas have been systematically surveyed and the locations of seafloor features are noticeably offset on different tracks (Fig. 8c,d). To resolve this issue

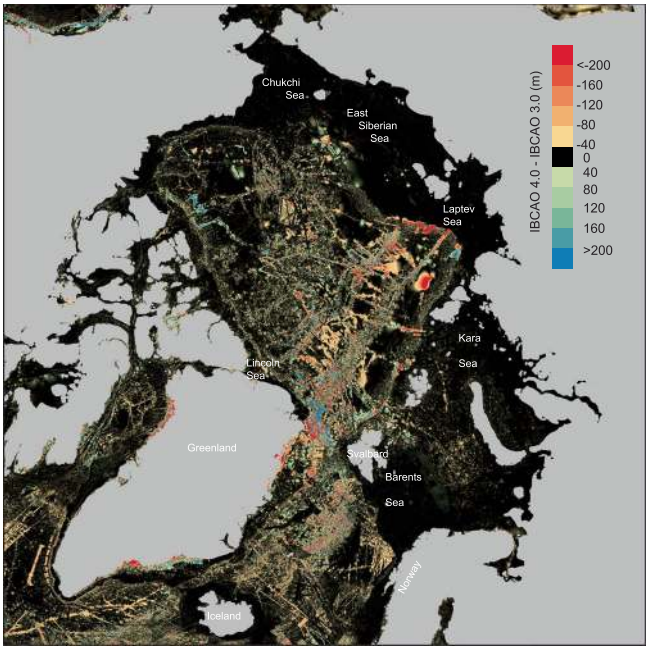

Fig. 5 Map showing the difference in meters between IBCAO Ver. 3.0 and 4.0, generated by subtracting Ver. 3.0 from 4.0. Positive values imply shallower depths in IBCAO Ver. 3.0 and vice versa.

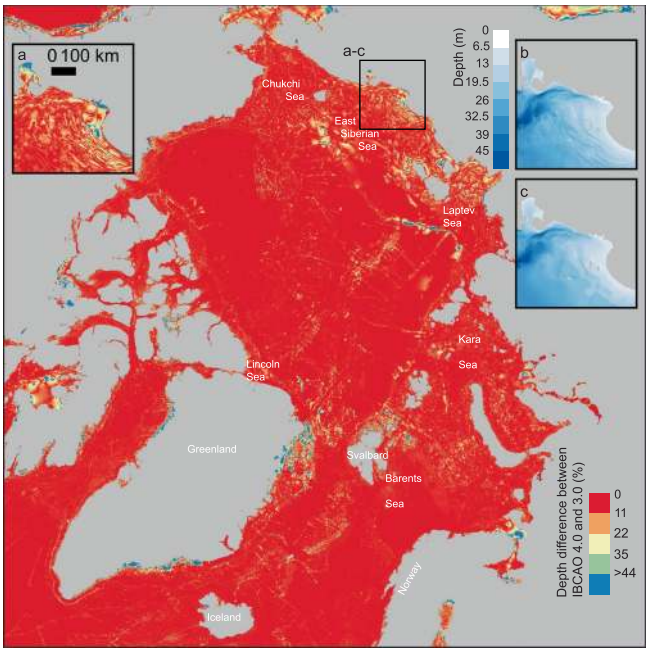

Fig. 6 Map showing the depth difference in percent between IBCAO Ver. 3.0 and 4.0 (i.e. the absolute depth difference between Ver. 4.0 and 3.0 divided by the absolute depth of Ver. 4.0). This reveals the updates in the shallow areas of the grid (i.e. mainly the large continental shelf areas). (**a**) Zoom-in on an area in the East Siberian Sea showing that substantially more details are distinguishable in IBCAO Ver. 4.0 (shown in **b**) compared to Ver. 3.0 (shown in **c**).

in areas that were based solely on SCICEX/SCAMP bathymetry and appeared to show large 'fault offsets', we used multibeam surveys that cross over the SCICEX tracks to re-position the swath data (Fig. 8c,d). These multibeam surveys were positioned using modern GPS implying a User Range Error (URE) commonly not exceeding 10 m. The result is not perfect but is a significant improvement in IBCAO Ver. 4.0 compared to Ver. 3.0.

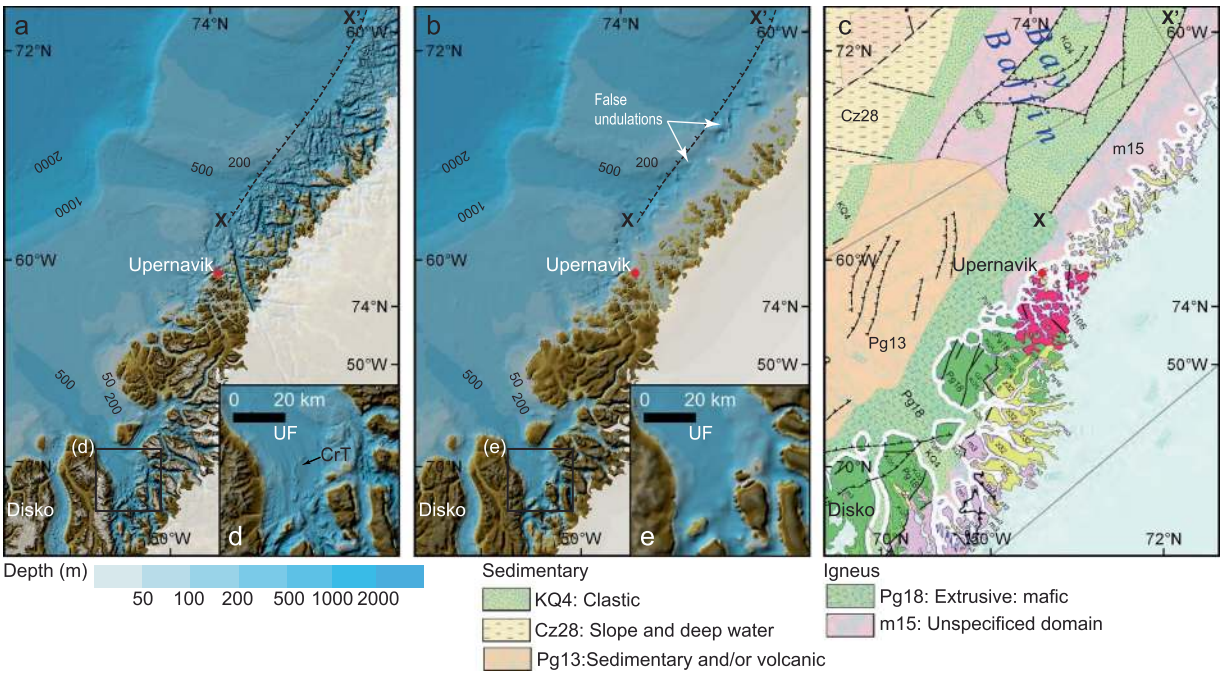

Fig. 7 Comparison off western Greenland between IBCAO Ver. 4.0 **(a)**, Ver. 3.0 **(b)** and the geological map by Harrison, *et al.*[34] **(c)**. The thrust fault marked X-X' on the geological map is shown as a reference on the bathymetric maps in **(a,b)**. The seafloor morphology changes markedly across the marked thrust fault in Ver. 4.0. The inset **(d)** shows how subglacial landforms in the form of Crag-and-Tails (CrT) are visible in Ver. 4, whereas they are not in Ver. 3.0 **(e)**. UF: Uummannaq Fjord. See location in Fig. 1.

Errors. Despite the fact that the IBCAO Ver. 4.0 DBM is a substantial improvement over previous versions, it is certainly not free of errors. The DBM remains limited by its underlying source database. The uncertainties associated with the depths of grid cells depend on a variety of factors including the approach used to correct soundings for sound speed, vertical referencing, navigation, and echo-sounder uncertainties. In addition, the gridding process will affect the final depth assigned to each grid cell. The random error component is thus a difficult parameter to derive, primarily because of lack of metadata on the widely varying data sources and the fact that some contributions are in the form of gridded compilations. In several areas we still rely on digitized contours from published maps for which the underlying source data are unknown. While the random error component of DBMs have been estimated using statistical modeling approaches[41,42], we do not provide this for IBCAO Ver. 4.0 because the metadata are not sufficient to provide a classification to a large enough portion of the database. Instead, the accompanying TIDs and SIDs provide information that is useful for users when addressing the reliability of IBCAO Ver. 4.0. In addition, we have assembled two grids aimed to further assist users in assessing the reliability of the DBM: minimum and maximum depth grids. These grids report the minimum and maximum depth value for each grid cell, implying a depth range where the block median filter had several input depth values in one grid cell.

Usage Notes

The most common uses of the IBCAO DBM are map-making and/or geospatial analyses using GIS software and other tools capable of displaying geographic information. The DBM is provided in netCDF and GeoTIFF formats, which are readily imported into most standard GIS software, for example QGIS and ArcMap. The 'x' and 'y' variables within the netCDF/GeoTIFF grid files represent the grid cell positions, along the x and y axis, in Polar Stereographic projection coordinates (meters), with a true scale set at 75°N. For the DBM, the 'z' value represents elevation in meters, depths below the sea surface are negative and heights above the sea surface are positive. The horizontal datum for the dataset is WGS 84 and the vertical datum can be assumed to be Mean Sea Level (however, note that there may be vertical reference issues for older observations, which may be due to chart datum). For the TID grid, the 'band 1' value represents the TID code, describing the type of data on which the corresponding cell in the DBM grid is based. A list of TID codes is given in Table 1. The projection parameters are provided in the European Petroleum Survey Group (EPSG) database (https://epsg.io/) as code 3996. This database is used by standard GIS software implying that searching for EPSG 3996, or IBCAO, will provide the correct projection and datum for the IBCAO DBM.

The Polar Stereographic coordinates can be converted to geographic using the GMT command *mapproject* with the following parameters:

mapproject [*input_lonlat*] -R-180/180/0/90 -Js0/90/75/1:1 -C -F > [*output_ xy*]

where *input_lonlat* is a table with longitude and latitude geographic coordinates and *output_xy* is a table with the resulting converted xy Polar Stereographic coordinates. The inverse conversion from xy to geographic

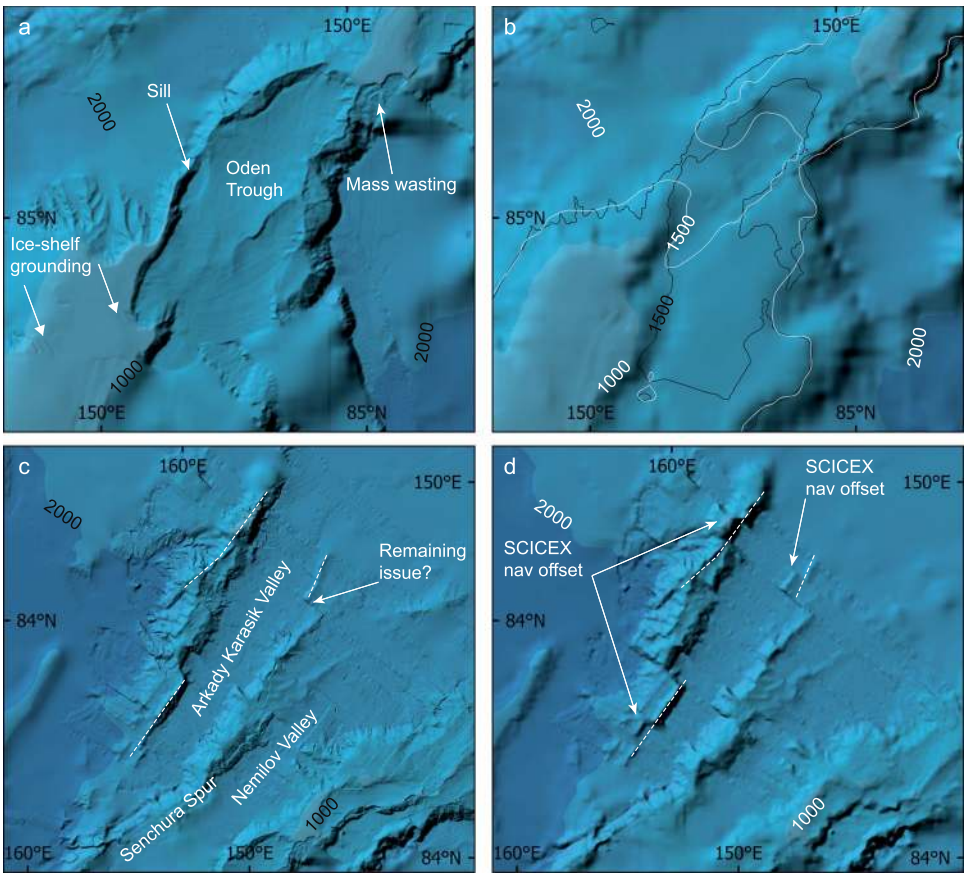

Fig. 8 Comparison between IBCAO Ver. 3.0 and Ver. 4.0 in two areas of the Lomonosov Ridge (Fig. 1). (**a**) Systematic multibeam surveys in 2014 by Swedish icebreaker *Oden* mapped a trough formed in the ridge crest, *Oden Trough*, and a critical sill depth influencing water exchange across the ridge[6]. In addition, lineations were mapped on the ridge crest, interpreted to be formed by a grounded ice shelf during the penultimate glaciation at about 140 000 years ago[37]. None of these features could be seen in IBCAO Ver. 3.0 (**b**) because it was compiled in this area through gridding of bathymetric contours retrieved from the Russian map "Bottom relief of the Arctic Ocean"[43]. The 1500 m isobaths derived from Ver. 3.0 (white) and 4.0 (black) shown in b clearly illustrate the large bathymetric differences between the two versions in the area of the sill. (**c**) The portrayal of the two spurs extending from the Lomonosov Ridge at about 84°N 155–160°E, one of them named Senchura Spur, are improved in Ver. 4.0 compared to Ver. 3.0 (**d**) due to additional multibeam bathymetry and adjustment of navigational issues in SCICEX 1999 (see main text).

coordinates is achieved by adding -I to the command above. See http://gmt.soest.hawaii.edu/doc/latest/mapproject.html for more information.

The GDAL command *gdaltransform* can also be used to convert between the Polar Stereographic and geographic coordinates by calling for the EPSG codes 3996 (IBCAO Polar Stereographic) and 4326 (WGS 84 geographic):

gdaltransform -s_srs EPSG:4326 -t_srs EPSG:3996

The inverse conversion is simply achieved by swapping the order of the EPSG codes. See https://gdal.org/programs/gdaltransform.html for more information.

Disclaimer information. Version 4.0 of the International Bathymetric Chart of the Arctic Ocean (IBCAO) grid, now referred to as the 'IBCAO Ver. 4.0 Grid', is available from https://www.gebco.net/. It is provided on behalf of the IBCAO project under the terms of the disclaimer information as given below.

The IBCAO Ver. 4.0 Grid, should NOT be used for navigation or for any other purpose involving safety at sea. The IBCAO Ver. 4.0 Grid is made available 'as is'. While every effort has been made to ensure reliability within the limits of present knowledge, the accuracy and completeness of the IBCAO Ver. 4.0 Grid cannot be guaranteed. No responsibility can be accepted by those involved in its creation or publication for any consequential loss, injury or damage arising from its use or for determining the fitness of the IBCAO Ver. 4.0 Grid for any particular use. The IBCAO Ver. 4.0 Grid is based on bathymetric data from many different sources of varying quality and coverage. As the IBCAO Ver. 4.0 Grid is an information product created by interpolation of measured data, the resolution of the IBCAO Ver. 4.0 Grid may be significantly different to that of the resolution of the underlying measured data.

Code availability

The gridding and statistical calculation procedures described in the Methods section are based on open source routines, provided within GMT (https://www.generic-mapping-tools.org/) and GDAL (https://gdal.org/), embedded in Python scripts. Codes are available upon request.

Received: 16 March 2020; Accepted: 14 May 2020;
Published online: 09 July 2020

References

1. Chandler, B. M. P. *et al*. Glacial geomorphological mapping: A review of approaches and frameworks for best practice. *Earth-Science Reviews* **185**, 806–846, https://doi.org/10.1016/j.earscirev.2018.07.015 (2018).
2. Stokes, C. R. *et al*. On the reconstruction of palaeo-ice sheets: Recent advances and future challenges. *Quaternary Science Reviews* **125**, 15–49, https://doi.org/10.1016/j.quascirev.2015.07.016 (2015).
3. Jakobsson, M., Mayer, L. A. & Monahan, D. Arctic Ocean Bathymetry: A Necessary Geospatial Framework. *2015* **68**, https://doi.org/10.14430/arctic4451 (2015).
4. Wölfl, A.-C. *et al*. Seafloor Mapping – The Challenge of a Truly Global Ocean Bathymetry. *Frontiers in Marine Science* **6**, https://doi.org/10.3389/fmars.2019.00283 (2019).
5. Timmermans, M.-L., Winsor, P. & Whitehead, J. A. Deep-Water Flow over the Lomonosov Ridge in the Arctic Ocean. *Journal of Physical Oceanography* **35**, 1489–1493, https://doi.org/10.1175/jpo2765.1 (2005).
6. Björk, G. *et al*. Bathymetry and oceanic flow structure at two deep passages crossing the Lomonosov Ridge. *Ocean Sci.* **14**, 1–13, https://doi.org/10.5194/os-14-1-2018 (2018).
7. Nghiem, S. V., Clemente-Colón, P., Rigor, I. G., Hall, D. K. & Neumann, G. Seafloor control on sea ice. *Deep Sea Research Part II: Topical Studies in Oceanography* **77–80**, 52–61, https://doi.org/10.1016/j.dsr2.2012.04.004 (2012).
8. Fenty, I. *et al*. Oceans Melting Greenland: Early Results from NASA's Ocean-Ice Mission in Greenland. *Oceanography* **29**, 71–83, https://doi.org/10.5670/oceanog.2016.100 (2016).
9. Davies, D. *et al*. High-resolution sub-ice-shelf seafloor records of twentieth century ungrounding and retreat of Pine Island Glacier, West Antarctica. *Journal of Geophysical Research: Earth Surface* **122**, 1698–1714, https://doi.org/10.1002/2017jf004311 (2017).
10. Batchelor, C. L., Dowdeswell, J. A., Rignot, E. & Millan, R. Submarine Moraines in Southeast Greenland Fjords Reveal Contrasting Outlet-Glacier Behavior since the Last Glacial Maximum. *Geophysical Research Letters* **46**, 3279–3286, https://doi.org/10.1029/2019gl082556 (2019).
11. Slabon, P. *et al*. Greenland ice sheet retreat history in the northeast Baffin Bay based on high-resolution bathymetry. *Quaternary Science Reviews* **154**, 182–198, https://doi.org/10.1016/j.quascirev.2016.10.022 (2016).
12. Mayer, L. A. In *Arctic* Science, I*nternational Law and Climate Change: Legal Aspects of Marine Science in the Arctic Ocean* (eds Susanne Wasum-Rainer, Ingo Winkelmann, & Katrin Tiroch) 83–95 (Springer Berlin Heidelberg, 2012).
13. Macnab, R. & Grikurov, G. Report: Arctic Bathymetry Workshop. 38 (Institute for Geology and Mineral Resources of the Ocean (VNIIOkeangeologia), St. Petersburg, Russia, 1997).
14. Jakobsson, M. *et al*. An improved bathymetric portrayal of the Arctic Ocean: Implications for ocean modeling and geological, geophysical and oceanographic analyses. *Geophysical Research Letters* **35**, L07602, https://doi.org/10.1029/2008gl033520 (2008).
15. Jakobsson, M. *et al*. The International Bathymetric Chart of the Arctic Ocean (IBCAO) Version 3.0. *Geophysical Research Letters* **39**, L12609, https://doi.org/10.1029/2012gl052219 (2012).
16. Jakobsson, M., Cherkis, N., Woodward, J., Macnab, R. & Coakley, B. New grid of Arctic bathymetry aids scientists and mapmakers. *EOS, Transactions American Geophysical Union* **81**, 89, 93, 96, https://doi.org/10.1029/00EO00059 (2000).
17. Smith, W. H. F. & Wessel, P. Gridding with continuous curvature splines in tension. *Geophysics* **55**, 293–305 (1990).
18. Macnab, R. & Jakobsson, M. Something Old, Something New: Compiling Historic and Contemporary Data to Construct Regional Bathymetric Maps, with the Arctic Ocean as a Case Study. *The International Hydrographic Review* **1**, 1–16 (2000).
19. Mayer, L. A. *et al*. The Nippon Foundation—GEBCO Seabed 2030 Project: The Quest to See the World's Oceans Completely Mapped by 2030. *Geosciences* **8**, 63, https://doi.org/10.3390/geosciences8020063 (2018).
20. GEBCO Compilation Group. GEBCO 2019 Grid, https://doi.org/10.5285/836f016a-33be-6ddc-e053-6c86abc0788e (2019).
21. Morlighem, M. *et al*. BedMachine v3: Complete Bed Topography and Ocean Bathymetry Mapping of Greenland From Multibeam Echo Sounding Combined With Mass Conservation. *Geophysical Research Letters* **44**, 11,051–011,061, https://doi.org/10.1002/2017GL074954 (2017).
22. EMODnet Bathymetry Consortium. EMODnet Digital Bathymetry (DTM), European Marine Observation and Data Network, https://doi.org/10.12770/18ff0d48-b203-4a65-94a9-5fd8b0ec35f6 (2018).
23. Wessel, P. & Smith, W. H. F. Free software helps map and display data. *EOS Transactions, American Geophysical Union* **72**(441), 445–446 (1991).
24. Smith, W. H. F. & Sandwell, D. T. Global seafloor topography from satellite altimetry and ship depth soundings. *Science* **277**, 1957–1962, https://doi.org/10.1126/science.277.5334.1956 (1997).
25. QGIS Geographic Information System. Open Source Geospatial Foundation Project v. 3.4.1-Madeira (2018).
26. IBCAO Version 4.0 Compilation Group. The International Bathymetric Chart of the Arctic Ocean (IBCAO) Version 4.0. *British Oceanographic Data Centre, National Oceanography Centre, NERC, UK*, https://doi.org/10.5285/a01d292f-b4a0-1ef7-e053-6c86abc0a4b2 (2020).
27. Schaffer, J. *et al*. A global, high-resolution data set of ice sheet topography, cavity geometry, and ocean bathymetry. *Earth Syst. Sci. Data* **8**, 543–557, https://doi.org/10.5194/essd-8-543-2016 (2016).
28. Arndt, J. E. *et al*. A new bathymetry of the Northeast Greenland continental shelf: Constraints on glacial and other processes. *Geochemistry, Geophysics, Geosystems* **16**, 3733–3753, https://doi.org/10.1002/2015GC005931 (2015).
29. Batchelor, C. L., Dowdeswell, J. A. & Rignot, E. Submarine landforms reveal varying rates and styles of deglaciation in North-West Greenland fjords. *Marine Geology* **402**, 60–80, https://doi.org/10.1016/j.margeo.2017.08.003 (2018).
30. Jakobsson, M. *et al*. The Holocene retreat dynamics and stability of Petermann Glacier in northwest Greenland. *Nature Communications* **9**, 2104, https://doi.org/10.1038/s41467-018-04573-2 (2018).
31. An, L., Rignot, E., Millan, R., Tinto, K. & Willis, J. Bathymetry of Northwest Greenland Using "Ocean Melting Greenland" (OMG) High-Resolution Airborne Gravity and Other Data. *Remote Sensing* **11**, 131, https://doi.org/10.3390/rs11020131 (2019).
32. An, L. *et al*. Bathymetry of Southeast Greenland from Ocean Melting Greenland (OMG) data. *Geophysical Research Letters* **46**, 11197–11205, https://doi.org/10.1029/2019gl083953 (2019).
33. Danielson, S. L. *et al*. Sounding the northern seas. *EOS* **96**, https://doi.org/10.1029/2015EO040975 (2015).
34. Harrison, J. C. *et al*. Geological Map of the Arctic: Map 2159A. 10.4095/287868 (2011).
35. Dowdeswell, J. A. *et al*. Late Quaternary ice flow in a West Greenland fjord and cross-shelf trough system: submarine landforms from Rink Isbrae to Uummannaq shelf and slope. *Quaternary Science Reviews* **92**, https://doi.org/10.1016/j.quascirev.2013.09.007 (2014).
36. Johnson, G. L., Monahan, D., Grönlie, G. & Sobczak, L. Sheet 5.17. *General Bathymetric Chart of the Oceans (GEBCO)* (1979).

37. Jakobsson, M. *et al*. Evidence for an ice shelf covering the central Arctic Ocean during the penultimate glaciation. *Nature Communication* **7**, 1–10, https://doi.org/10.1038/ncomms10365 (2016).
38. Marcussen, C., Mørk, F., Funck, T., Weng, W. L. & Pedersen, M. In *Geological Survey of Denmark and Greenland Bulletin* Vol. 33 41–44 (2015).
39. Edwards, M. H. & Coakley, B. J. SCICEX Investigations of the Arctic Ocean System. *Chemie der Erde* **63**, 281–328, https://doi.org/10.1078/0009-2819-00039 (2003).
40. Armstrong, A., Mayer, L. A. & Gardner, J. V. Seamounts, submarine channels, and new discoveries: Benefits of continental shelf surveys extend beyond defining the limits of the shelf. *Journal of Ocean Technology* **10**, 1–14 (2015).
41. Elmore, P. A., Fabre, D. H., Sawyer, R. T. & Ladner, R. W. Uncertainty estimation for databased bathymetry using a Bayesian network approach. *Geochem. Geophys. Geosyst.* **13**, Q09011, https://doi.org/10.1029/2012gc004144 (2012).
42. Jakobsson, M., Calder, B. & Mayer, L. A. On the effect of random errors in gridded bathymetric compilations. *Journal of geophysical research* **107**, 1–11, https://doi.org/10.1029/2001JB000616 (2002).
43. Naryshkin, G. Bottom relief of the Arctic Ocean. Bathymetric contour map (2001).
44. Zimmermann, M., Prescott, M. M. & Haeussler, P. J. Bathymetry and Geomorphology of Shelikof Strait and the Western Gulf of Alaska. *Geosciences* **9**, 409, https://doi.org/10.3390/geosciences9100409 (2019).
45. Prescott, M. M. & Zimmermann, M. Smooth sheet bathymetry of Norton Sound. Report No. Memo. NMFS-AFSC-298, 23 (U.S. Department of Commerce, 2015).
46. Zimmermann, M. & Prescott, M. M. Smooth sheet bathymetry of Cook Inlet, Alaska. Report No. Memo. NMFS-AFSC-275, 32 (U.S. Department of Commerce, 2014).
47. Zimmermann, M., Prescott, M. M. & Rooper, C. N. Smooth sheet bathymetry of the Aleutian Islands. Report No. Memo. NMFS-AFSC-250, 43 (U.S. Department of Commerce, 2013).
48. Rebesco, M. *et al*. Deglaciation of the western margin of the Barents Sea Ice Sheet - A swath bathymetric and sub-bottom seismic study from the Kveithola Trough. *Marine Geology* **279**, 141–147, https://doi.org/10.1016/j.margeo.2010.10.018 (2011).
49. Pedrosa, M. T. *et al*. Seabed morphology and shallow sedimentary structure of the Storfjorden and Kveithola trough-mouth fans (North West Barents Sea). *Marine Geology* **286**, 65–81, https://doi.org/10.1016/j.margeo.2011.05.009 (2011).
50. Rui, L. *et al*. Geomorphology and development of a high-latitude channel system: the INBIS channel case (NW Barents Sea, Arctic). *Arktos* **5**, 15–29, https://doi.org/10.1007/s41063-019-00065-9 (2019).
51. Bensi, M. *et al*. Deep Flow Variability Offshore South-West Svalbard (Fram Strait). *Water* **11**, 683, https://doi.org/10.3390/w11040683 (2019).
52. Hanebuth, T. J. J., Rebesco, M., Urgeles, R., Lucchi, R. G. & Freudenthal, T. Drilling Glacial Deposits in Offshore Polar Regions. *Eos, Transactions American Geophysical Union* **95**, 277–278, https://doi.org/10.1002/2014eo310001 (2014).
53. Andreassen, K. *et al*. Barents Sea and the West Spitsbergen Margin, UiT 2009: Marine Geophysical/Geological Cruise to Outer Bear Island trough, Kveithola trough and the West Spitsbergen Margin. 33 (University of Tromsø, 2009).
54. Rüther, D. C. *et al*. Pattern and timing of the northwestern Barents Sea Ice Sheet deglaciation and indications of episodic Holocene deposition. *Boreas* **41**, 494–512, https://doi.org/10.1111/j.1502-3885.2011.00244.x (2012).
55. Ivaldi, R., Demarte, M. & HIGH NORTH 17 Team. High North 17 Cruise Report. 68 (Istituto Idrografico della Marina, 2017).
56. Ivaldi, R., Demarte, M. & High North 18 Team. High North 18 Cruise Report. Arctic Marine Geophysical Campaign. 99 (Istituto Idrografico della Marina, 2018).
57. Hogan, K. A. *et al*. Submarine landforms and ice-sheet flow in the Kvitøya Trough, northwestern Barents Sea. *Quaternary Science Reviews* **29**, 3545–3562, https://doi.org/10.1016/j.quascirev.2010.08.015 (2010).
58. Dowdeswell, J. A. *et al*. Past ice-sheet flow east of Svalbard inferred from streamlined subglacial landforms. *Geology* **38**, 163–166, https://doi.org/10.1130/g30621.1 (2010).
59. Westbrook, G. K. *et al*. Escape of methane gas from the seabed along the West Spitsbergen continental margin. *Geophys. Res. Lett.* **36**, L15608, https://doi.org/10.1029/2009gl039191 (2009).
60. Cherkis, N. Z. *et al*. Bathymetry of the Barents and Kara Seas. *Geological Society of America Map and Chart Series*, Bathymetry of the Barents and Kara Seas (1991).
61. Matishov, G. G., Cherkis, N. Z., Vermillion, M. S. & Forman, S. L. Bathymetry of the Franz Josef Land Area. *Geological Society of America Map and Chart Series*, Bathymetry of the Franz Josef Land area (1995).
62. Naryshkin, G. Bottom relief of the Arctic Ocean. Bathymetric contour map (1999).
63. Perry, R. K. *et al*. Bathymetry of the Arctic Ocean. *Geological Society of America Map and Chart Series* (1986).
64. Zayonchek, A. V. *et al*. In *Contribution of Russia to International Polar Year* Vol. 4 (ed. Paulsen, M.) Ch. Structure and evolution of the Lithosphere, 111–157 (2010).
65. Jackson, H. R. Field report for 2007 the CCGS Louis S. St-Laurent seismic cruise to the Canada Basin. 143 (Geological Survey of Canada, Natural Resources Canada, 2008).
66. Jackson, H. R. & DesRoches, K. J. 2008 Louis S. St-Laurent Field Report, August 22 – October 3, 2008. 184 (Geological Survey of Canada, Natural Resources Canada, 2010).
67. Mosher, D. C., Shimeld, J. D. & Hutchinson, D. R. 2009 Canada Basin seismic reflection and refraction survey, western Arctic Ocean: CCGS Louis S. St-Laurent expedition report. 266 (Geological Survey of Canada, Geological Survey of Canada, Ottawa, Ontario, 2009).
68. Mosher, D. C., Shimeld, J. & Champman, B. C. Canada Basin seismic reflection and refraction survey, western Arctic Ocean: CCGS Louis S. St-Laurent expedition report. 240 (Geological Survey of Canada, Geological Survey of Canada, Ottawa, Ontario, 2011).
69. Mosher, D. C. 2011 Canadian High Arctic Seismic Expedition: CCGS Louis S. St-Laurent expedition report. 290 (Geological Survey of Canada, Geological Survey of Canada, Ottawa, Ontario, 2012).
70. Travaglini, P. G. Final Field Report: Arctic Survey - UNCLOS 2014. 82 (Canadian Hydrographic Survey, Natural Resources Canada, 2014).
71. Youngblut, S. Final Field Report: Amundsen Basin Survey: UNCLOS 2015. 37 (Canadian Hydrographic Survey, Natural Resources Canada, 2015).
72. Gårdfeldt, K. & Lindgren, Å. SWEDARCTIC Arctic Ocean 2016: Expedition Report. 1–117 (Stockholm: Swedish Polar Research Secretariat, 2017).
73. Jakobsson, M., Marcussen, C. & LOMROG, S. P. Lomonosov Ridge Off Greenland 2007 (LOMROG) - Cruise Report. 122 (Geological Survey of Denmark and Greenland, Copenhagen, 2008).
74. Jakobsson, M. *et al*. An Arctic Ocean ice shelf during MIS 6 constrained by new geophysical and geological data. *Quaternary Science Reviews* **29**, 3505–3517, https://doi.org/10.1016/j.quascirev.2010.03.015 (2010).
75. Marcussen, C. & LOMROG II Scientific Party. Lomonosov Ridge Off Greenland 2009 (LOMROG II) - Cruise Report. 151 (Geological Survey of Denmark and Greenland, Ministry of Climate and Energy, 2011).
76. Marcussen, C. & LOMROG III Scientific Party. Lomonosov Ridge Off Greenland 2012 (LOMROG III) - Cruise Report. 220 (Geological Survey of Denmark and Greenland, Geological Survey of Denmark and Greenland, Ministry of Climate and Energy, 2012).
77. Marcussen, C. & EAGER 2011 Scientific Party. East Greenland Ridge 2011 (EAGER) - Cruise Report. 1–86 (Geological Survey of Denmark and Greenland, Ministry of Climate and Energy, Copenhagen, 2011).

78. Kågesten, G., Fiorentino, D., Baumgartner, F. & Zillén, L. How Do Continuous High-Resolution Models of Patchy Seabed Habitats Enhance Classification Schemes? *Geosciences* **9**, 237, https://doi.org/10.3390/geosciences9050237 (2019).
79. Schumann, K., Völker, D. & Weinrebe, W. R. Acoustic mapping of the Ilulissat Ice Fjord mouth, West Greenland. *Quaternary Science Reviews* **40**, 78–88, https://doi.org/10.1016/j.quascirev.2012.02.016 (2012).
80. Kang, S.-H., Nam, S.-i., Yim, J. H., Chung, K. H. & Hong, J. K. Cruise Report: RV Araon ARA03B. 174 (Korea Polar Research Institute (KOPRI), 2012).
81. Kristoffersen, Y. & Hall, J. K. Hovercraft as a Mobile Science Platform Over Sea Ice in the Arctic Ocean. *Oceanography* **27**, 170–179, https://doi.org/10.5670/oceanog.2014.33 (2014).
82. Rignot, E. *et al*. Bathymetry data reveal glaciers vulnerable to ice-ocean interaction in Uummannaq and Vaigat glacial fjords, west Greenland. *Geophysical Research Letters* **43**, 2667–2674, https://doi.org/10.1002/2016GL067832 (2016).
83. An, L., Rignot, E., Mouginot, J. & Millan, R. A Century of Stability of Avannarleq and Kujalleq Glaciers, West Greenland, Explained Using High-Resolution Airborne Gravity and Other Data. *Geophysical Research Letters* **45**, 3156–3163, https://doi.org/10.1002/2018gl077204 (2018).
84. An, L. *et al*. Bed elevation of Jakobshavn Isbræ, West Greenland, from high-resolution airborne gravity and other data. *Geophysical Research Letters* **44**, 3728–3736, https://doi.org/10.1002/2017gl073245 (2017).
85. Millan, R. *et al*. Vulnerability of Southeast Greenland Glaciers to Warm Atlantic Water From Operation IceBridge and Ocean Melting Greenland Data. *Geophysical Research Letters* **45**, 2688–2696, https://doi.org/10.1002/2017gl076561 (2018).
86. Rignot, E. *et al*. Modeling of ocean-induced ice melt rates of five west Greenland glaciers over the past two decades. *Geophysical Research Letters* **43**, 6374–6382, https://doi.org/10.1002/2016gl068784 (2016).
87. Rignot, E., Fenty, I., Xu, Y., Cai, C. & Kemp, C. Undercutting of marine-terminating glaciers in West Greenland. *Geophysical Research Letters* **42**, 5909–5917, https://doi.org/10.1002/2015gl064236 (2015).
88. Wood, M. *et al*. Ocean-Induced Melt Triggers Glacier Retreat in Northwest Greenland. *Geophysical Research Letters* **45**, 8334–8342, https://doi.org/10.1029/2018gl078024 (2018).
89. Coakley, B. & Ilhan, I. & Chukchi Edges Science Party. In *American Geophysical Union Fall Meeting 2011* Abstract T33A-2365 (American Geophysical Union, San Fransisco, USA, 2011).
90. Dove, D., Polyak, L. & Coakley, B. Widespread, multi-source glacial erosion on the Chukchi margin, Arctic Ocean. *Quaternary Science Reviews* **92**, 112–122, https://doi.org/10.1016/j.quascirev.2013.07.016 (2014).
91. Reece, R. S. *et al*. The role of farfield tectonic stress in oceanic intraplate deformation, Gulf of Alaska. *Journal of Geophysical Research: Solid Earth* **118**, 1862–1872, https://doi.org/10.1002/jgrb.50177 (2013).
92. Anderson, L. G. *et al*. Water masses and circulation in the Eurasian Basin: Results from *Oden* 91 Expedition. *Journal of Geophysical Research* **99**, 3273–3283, https://doi.org/10.1029/93JC02977 (1994).
93. Jakobsson, M. First high-resolution chirp sonar profiles from the central Arctic Ocean reveal erosion of Lomonsov Ridge sediments. *Marine Geology* **158**, 111–123, https://doi.org/10.1016/S0025-3227(98)00186-8 (1999).
94. Björk, G., Söderkvist, J., Winsor, P., Nikolopoulos, A. & Steele, M. Return of the cold halocline layer to the Amundsen Basin of the Arctic Ocean: Implications for the sea ice mass balance. *Geophysical Research Letters* **29**, 8-1–8-4, https://doi.org/10.1029/2001gl014157 (2002).
95. Sohn, R. A. *et al*. Explosive volcanism on the ultraslow-spreading Gakkel Ridge, Arctic Ocean. *Nature* **453**, 1236–1238, https://doi.org/10.1038/nature07075 (2008).
96. Freire, F., Gyllencreutz, R., Jafri, R. & Jakobsson, M. Acoustic evidence of a submarine slide in the deepest part of the Arctic, the Molloy Hole. *Geo-Marine Letters*, 315–325, https://doi.org/10.1007/s00367-014-0371-5 (2014).
97. The SWERUS Scientific Party. Cruise Report for SWERUS-C3 Leg 1. 200 (Bolin Centre for Climate Research, Stockholm, 2016).
98. The SWERUS Scientific Party. Cruise Report for SWERUS-C3 Leg 2. 190 (Bolin Centre for Climate Research, Stockholm, 2016).
99. Mix, A. C., Jakobsson, M. & Petermann-2015 Scientific Party. Petermann-2015 Expedition Launches International Collaboration in Arctic Science. *Witness the Arctic* (2015).
100. Freire, F. *et al*. High resolution mapping of offshore and onshore glaciogenic features in metamorphic bedrock terrain, Melville Bay, northwestern Greenland. *Geomorphology* **250**, 29–40, https://doi.org/10.1016/j.geomorph.2015.08.011 (2015).
101. Noormets, R., Dowdeswell, J. A., Jakobsson, M. & Ó Cofaigh, C. In *American Geophysical Union Fall Meeting, San Fransisco* C43C-0564 (American Geophysical Union, San Fransisco, 2010).
102. Fransner, O., Noormets, R., Chauhan, T., O'Regan, M. & Jakobsson, M. Late Weichselian ice stream configuration and dynamics in Albertini Trough, northern Svalbard margin. *arktos* **4**, 1, https://doi.org/10.1007/s41063-017-0035-6 (2018).
103. Fransner, O. *et al*. Glacial landforms and their implications for glacier dynamics in Rijpfjorden and Duvefjorden, northern Nordaustlandet, Svalbard. *Journal of Quaternary Science* **32**, 437–455, https://doi.org/10.1002/jqs.2938 (2017).
104. Fransner, O., Noormets, R., Flink, A. E., Hogan, K. A. & Dowdeswell, J. A. Sedimentary processes on the continental slope off Kvitøya and Albertini troughs north of Nordaustlandet, Svalbard – The importance of structural-geological setting in trough-mouth fan development. *Marine Geology* **402**, 194–208, https://doi.org/10.1016/j.margeo.2017.10.008 (2018).
105. Lockwood, C. *Reconstruction of ice stream retreat and palaeoceanographic development during the deglaciation and Holocene in the Storfjorden Trough, Svalbard* MSc thesis, UiT The Arctic University of Norway, (2016).
106. Mau, S. *et al*. Widespread methane seepage along the continental margin off Svalbard - from Bjørnøya to Kongsfjorden. *Scientific Reports* **7**, 42997, https://doi.org/10.1038/srep42997 (2017).
107. Mayer, L. A., Calder, B. & Mosher, D. U.S. Law of the Sea cruise to map the foot of the slope and 2500-m isobath of the US Arctic Ocean margin: CRUISE HEALY 1603. 135 (Center for Coastal and Ocean Mapping/Joint Hydrographic Center University of New Hampshire, Durham, New Hampshire, 2016).
108. Mayer, L. A. & Armstrong, A. A. U.S. Law of the Sea cruise to map the foot of the slope and 2500-m isobath of the US Arctic Ocean margin: CRUISE HEALY 1202. 159 (Center for Coastal and Ocean Mapping/Joint Hydrographic Center University of New Hampshire, Durham, New Hampshire, 2012).
109. Mayer, L. A. U.S. Law of the Sea cruise to map the foot of the slope and 2500-m isobath of the US Arctic Ocean margin: CRUISE HEALY 1102. 235 (Center for Coastal and Ocean Mapping/Joint Hydrographic Center University of New Hampshire, Durham, New Hampshire, 2011).
110. Mayer, L. A. U.S. Law of the Sea cruise to map the foot of the slope and 2500-m isobath of the US Arctic Ocean margin: CRUISE HE-0905. 118 (Center for Coastal and Ocean Mapping/Joint Hydrographic Center University of New Hampshire, Durham, New Hampshire, 2009).
111. Mayer, L. A. U.S. Law of the Sea cruise to map the foot of the slope and 2500-m isobath of the US Arctic Ocean margin: CRUISE HE-0805. 179 (Center for Coastal and Ocean Mapping/Joint Hydrographic Center University of New Hampshire, Durham, New Hampshire, 2008).
112. Mayer, L. A. & Armstrong, A. A. U.S. Law of the Sea cruise to map the foot of the slope and 2500-m isobath of the US Arctic Ocean margin: CRUISE HE-0703. 182 (Center for Coastal and Ocean Mapping/Joint Hydrographic Center University of New Hampshire, Durham, New Hampshire, 2007).
113. Mayer, L. A. U.S. Law of the Sea cruise to map the foot of the slope and 2500-m isobath of the US Arctic Ocean margin: CRUISES HE-0302. 19 (Center for Coastal and Ocean Mapping/Joint Hydrographic Center University of New Hampshire, Durham, New Hampshire, 2004).

114. Jakobsson, M. *et al*. Multibeam bathymetric and sediment profiler evidence for ice grounding on the Chukchi Borderland, Arctic Ocean, Arctic Ocean. *Quaternary Research* **63**, 150–160, https://doi.org/10.1016/j.yqres.2004.12.004 (2005).
115. Mayer, L. A. U.S. Law of the Sea cruise to map the foot of the slope and 2500-m isobath of the US Arctic Ocean margin: CRUISES HE-0405. 47 (Center for Coastal and Ocean Mapping/Joint Hydrographic Center University of New Hampshire, Durham, New Hampshire, 2005).
116. Darby, D., Jakobsson, M. & Polyak, L. Icebreaker Expedition Collects Key Arctic Sea Floor and Ice Data. *EOS Transactions, American Geophysical Union* **86**, 549–556, https://doi.org/10.1029/2005EO520001 (2005).
117. Newton, G. B. The Science Ice Exercise Program: History, achievment, and future of SCICEX. *Arctic Research of the United States* **14**, 2–7 (2000).

Acknowledgements

The compilation of the IBCAO DBM is a part of the Nippon-Foundation- GEBCO-Seabed 2030 project receiving funding from the Nippon Foundation of Japan. The authors are deeply indebted to a broad range of agencies and institutions that have funded the collection of bathymetric data in the Arctic (see Online-only Table 2) and have agreed to contribute it to this compilation. Open access funding provided by Stockholm University.

Author contributions

Martin Jakobsson: Led the compilation work, writing of the data description, figure production. Larry A. Mayer: Co-Lead the compilation work, writing of the data description. Caroline Bringensparr: Processing and merging of provided source data, quality control. Carlos F. Castro: Processing and merging of provided source data, quality control. Rezwan Mohammad: Gridding and statistical calculation, development of compilation computer algorithms and data-management system, quality control. Paul Johnsson: Provided source data, quality control. Tomer Ketter: Provided source data, quality control. Daniela Accettella: Provided source data, quality control. David Amblas: Provided source data, quality control. Lu An: Provided source data, quality control. Jan Erik Arndt: Provided source data, quality control. Miquel Canals: Provided source data, quality control. José L. Casamor: Provided source data, quality control. Nolwenn Chauche: Provided source data, quality control. Bernard Coakley: Provided source data, quality control. Seth Danielson: Provided source data, quality control. Maurizio Demarte: Provided source data, quality control. Mary-Lynn Dickson: Provided source data, quality control. Boris Dorschel: Provided source data, quality control. Julian A. Dowdeswell: Provided source data, quality control. Simon Dreutter: Provided source data, quality control. Alice C. Fremand: Provided source data, quality control. Dana Gallant: Provided source data, quality control. John K. Hall: Provided source data, quality control. Laura Hehemann: Provided source data, quality control. Hanne Hodnesdal: Provided source data, quality control. Jongkuk Hong: Provided source data, quality control. Roberta Ivaldi: Provided source data, quality control. Emily Kane: Provided source data, quality control. Ingo Klaucke: Provided source data, quality control. Diana W. Krawczyk: Provided source data, quality control. Yngve Kristoffersen: Provided source data, quality control. Boele R. Kuipers: Provided source data, quality control. Giuseppe Masetti: Provided source data, quality control. Romain Millan: Provided source data, quality control. Mathieu Morlighem: Provided source data, quality control. Riko Noormets: Provided source data, quality control. Megan M. Prescott: Provided source data, quality control. Michele Rebesco: Provided source data, quality control. Eric Rignot: Provided source data, quality control. Igor Semiletov: Provided source data, quality control. Alex J. Tate: Provided source data, quality control. Paola Travaglini: Provided source data, quality control. Isabella Velicogna: Provided source data, quality control. Pauline Weatherall: Provided source data, quality control. Wilhem Weinrebe: Provided source data, quality control. Joshua K. Willis: Provided source data, quality control. Michael Wood: Provided source data, quality control. Yulia Zarayskaya: Provided source data, quality control. Tao Zhang: Provided source data, quality control. Mark Zimmermann: Provided source data, quality control. Karl B. Zinglersen: Provided source data, quality control.

Competing interests

The authors declare no competing interests.

Additional information

Correspondence and requests for materials should be addressed to M.J. or L.A.M.

Reprints and permissions information is available at www.nature.com/reprints.

Publisher's note Springer Nature remains neutral with regard to jurisdictional claims in published maps and institutional affiliations.

Martin Jakobsson[1,2]✉, Larry A. Mayer[3]✉, Caroline Bringensparr[1,2], Carlos F. Castro[1,2], Rezwan Mohammad[1,2], Paul Johnson[3], Tomer Ketter[3], Daniela Accettella[4], David Amblas[5], Lu An[6], Jan Erik Arndt[7], Miquel Canals[5], José Luis Casamor[5], Nolwenn Chauché[8], Bernard Coakley[9], Seth Danielson[10], Maurizio Demarte[11], Mary-Lynn Dickson[12], Boris Dorschel[7], Julian A. Dowdeswell[13], Simon Dreutter[7], Alice C. Fremand[14], Dana Gallant[15], John K. Hall[16], Laura Hehemann[7], Hanne Hodnesdal[17], Jongkuk Hong[18], Roberta Ivaldi[11], Emily Kane[6], Ingo Klaucke[19], Diana W. Krawczyk[20,21], Yngve Kristoffersen[22], Boele R. Kuipers[17], Romain Millan[23], Giuseppe Masetti[24], Mathieu Morlighem[6], Riko Noormets[25], Megan M. Prescott[26], Michele Rebesco[4], Eric Rignot[6,27], Igor Semiletov[28,29], Alex J. Tate[14], Paola Travaglini[30], Isabella Velicogna[6,27], Pauline Weatherall[31], Wilhelm Weinrebe[19], Joshua K. Willis[27], Michael Wood[6], Yulia Zarayskaya[32], Tao Zhang[33], Mark Zimmermann[34] & Karl B. Zinglersen[20]

[1]Department of Geological Sciences, Stockholm University, Stockholm, Sweden. [2]Bolin Centre for Climate Research, Stockholm University, 106 91, Stockholm, Sweden. [3]Center for Coastal and Ocean Mapping, University of New Hampshire, Durham, NH, USA. [4]National Institute of Oceanography and Applied Geophysics, Sgonico, Italy. [5]CRG Marine Geosciences, Department of Earth and Ocean Dynamics, University of Barcelona, Barcelona, Spain. [6]Department of Earth System Science, University of California, Irvine, CA, USA. [7]Alfred-Wegener-Institut, Helmholtz Centre for Polar and Marine Research, Bremerhaven, Germany. [8]Access Arctic, Le Vieux Marigny, France. [9]Geophysical Institute, University of Alaska, Fairbanks, AK, USA. [10]College of Fisheries and Ocean Sciences, University of Alaska, Fairbanks, AK, USA. [11]Italian Hydrographic Service, Genoa, Italy. [12]Geological Survey of Canada, Dartmouth, Nova Scotia, Canada. [13]Scott Polar Research Institute, University of Cambridge, Cambridge, UK. [14]UK Polar Data Centre, British Antarctic Survey, Cambridge, UK. [15]Canadian Hydrographic Service, Burlington, Ontario, Canada. [16]Geological Survey of Israel, Jerusalem, Israel. [17]Norwegian Mapping Authority, Hydrographic Service, Stavanger, Norway. [18]Korea Polar Research Institute, Incheon, South Korea. [19]GEOMAR Helmholtz Centre for Ocean Research Kiel, Kiel, Germany. [20]Greenland Institute of Natural Resources, Nuuk, Greenland. [21]Geological Survey of Denmark and Greenland, Copenhagen, Denmark. [22]Department of Earth Science, University of Bergen, Bergen, Norway. [23]Institut des Geosciences de l'Environment, Universite Grenoble Alpes, CNRS, Grenoble, France. [24]Danish Geodata Agency, Danish Hydrographic Office, Ålborg, Denmark. [25]University Centre in Svalbard, Svalbard, Norway. [26]Lynker Technologies, Seattle, USA. [27]Jet Propulsion Laboratory, California Institute of Technology, Pasadena, CA, USA. [28]Tomsk Polytechnic University, Tomsk, Russia. [29]Laboratory of Arctic Studies, V.I. Il'ichov Pacific Oceanological Institute, Far Eastern Branch of the Russian Academy of Sciences, Vladivostok, Russia. [30]Canadian Hydrographic Service, Darthmouth, Nova Scotia, Canada. [31]British Oceanographic Data Centre, Liverpool, UK. [32]Geological Institute, Russian Academy of Sciences, Moscow, Russian Federation. [33]Second Institute of Oceanography, Ministry of Natural Resources, Beijing, China. [34]NOAA National Marine Fisheries Service, Alaska Fisheries Science Center, Seattle, USA. ✉e-mail: martin.jakobsson@geo.su.se; larry.mayer@ccom.unh.edu